VI. Summary

The statistical behavior of instrument-limited phased array angular measurement errors has been examined with the aid of a specially developed computer program which simulates the effect of 1) beam steering computation accuracy, 2) truncation of beam steering commands, and 3) differential phase errors.

The following conclusions were reached for a typical array configuration (1891 elements):

1) A beam split ratio, neglecting bias errors, in excess of 300:1 can be achieved with only 3-bit phase shifters.

2) Truncation of row and steering commands to four bits reduces the beam split ratio to below 100:1.

3) Differential phase errors of 10° (one sigma per bit) only increased measurement errors about 20 percent.

4) A steering angle of approximately 2 ms in any direction will cause a 50 percent drop in the autocorrelation of the angular errors. The shape of the central peak of the two-dimensional autocorrelation function does not show strong "preferred" correlation directions.

5) The phase dithering technique was shown to be completely effective in annihilating all angle measurement error correlations. Results were presented for a typical sector scan, but beam steering is not required to achieve decorrelation. The phase dithering technique is very easy to implement. Frequency and beam dithering were also found to be effective decorrelation techniques, nearly as effective as phase dithering, but involve compromises which could make them unacceptable for certain applications.

Acknowledgment

A number of people were consulted during the course of this work; they provided the authors with valuable help and suggestions. In particular, the assistance of L. J. Cantafio, Radar and Communications Department, and C. Crummer, Information Processing Division, both of the Aerospace Corporation, are gratefully acknowledged. We acknowledge helpful discussions with J. Walsh, D. K. Barton, and others at the Raytheon Company, and L. Schwartzman and P. M. Liebman and others at the Sperry Gyroscope Company.

References

[1] D. K. Barton and H. R. Ward, *Handbook of Radar Measurement*. Englewood Cliffs, N. J.: Prentice Hall, 1969.
[2] W. J. Albersheim, "Reduction of side lobes and pointing errors in phased array radars by randomizing quantization steps," the Mitre Corp., Bedford, Mass., Rep. TM-3435, AD 402953, Apr. 1963.
[3] C. J. Miller, "Minimizing the effects of phase quantization errors in an electronically scanned array," in *Proc. 1964 Symp. Electronically Scanned Array Techniques and Applications*, RADC-TDR-64-225, vol. 1, pp. 17–38.
[4] D. R. Rhodes, *Introduction to Monopulse*. New York: McGraw-Hill, 1959.
[5] W. H. Nester, "A study of tracking accuracy in monopulse phased arrays," *IRE Trans. Antennas Propagat.*, pp. 237–246, May 1962.
[6] B. R. Hatcher, "Collimation of row-and-column steered phased arrays," *Proc. IEEE*, pp. 1787–1790, Nov. 1968.

Antenna Gain Calibration on a Ground Reflection Range

LELAND H. HEMMING and RAYMON A. HEATON

***Abstract*—The absolute gain of wide-beam antennas may be accurately measured using the method described. Both the theoretical and practical aspects of gain calibration on a ground reflection antenna range are presented. The measurement procedures developed were used to calibrate a log-periodic antenna at selected frequencies from 250 to 400 MHz. Measured data at 300 MHz is tabulated and error contributions are analyzed, yielding a measurement accuracy of ±0.27 dB with a 95 percent confidence interval.**

Manuscript received January 10, 1973; revised March 1, 1973.
L. H. Hemming is with the Scientific-Atlanta, Inc., Atlanta, Ga. 30324.
R. A. Heaton was with the Scientific-Atlanta, Inc., Atlanta, Ga. He is now with the Bishop Company, Huntsville, Ala.

I. Introduction

The MEASUREMENT of the gain[1] of narrow-beam antennas may be accomplished with reasonable accuracy using the gain comparison technique with available gain standards and a well designed antenna range. However, for frequencies below L band, gain standards are not generally available, with the exception of dipoles, whose low directivity often causes excessive measurement

[1] For the purposes of this discussion, antenna gain will be assumed to be the maximum gain of the antenna, hence the gain at the peak of the main lobe.

error. It is, therefore, necessary at these frequencies to consider the calibration of a gain standard with increased directivity if the measurement error is to be reduced.

The calibration of a gain standard is most frequently accomplished by the two-antenna method or the three-antenna method [1]–[3]. Both techniques are based on the Friis transmission formula [4] for power transfer between two antennas, which theoretically requires an infinite antenna separation and a free-space test environment. For gain calibration of antennas with narrow beamwidths this condition may be approached with an antenna range of sufficient length and tower heights which minimize reflections from the range surface. For wide-beam antennas, however, tower heights necessary to minimize range reflections become impractical and the antennas must be calibrated on a ground reflection antenna range.

II. Theory

The method described is directly applicable to antennas which respond only to the electric field. It would require modification to be used with loop or slot antennas, and further modification for antennas which may be a combination of electric and magnetic types. The basic test configuration is that shown in Fig. 1. Horizontal polarization was employed to avoid the wave tilt and rapid variation of reflection coefficient associated with vertically polarized waves reflected from the range surface (see [6, p. 635]).

The field at the receiving antenna is assumed to be the vector sum of the electric field due to the direct path contribution and that due to the contribution from the reflected path. The amplitude of the electric field at the receiving antenna due to the direct path wave is given by

$$E_D = K\left[P_0(K_1G_t)(K_2G_x)\left(\frac{\lambda}{4\pi R_D}\right)^2\right]^{1/2} \tag{1}$$

where

$$R_D = [R_0^2 + (h_r - h_t)^2]^{1/2}.$$

Equation (1) is the field equivalent of the Friis transmission formula [4]. The amplitude of the ground-reflection field at the receiving antenna is given by

$$E_r = K\left[P_0G_tG_r\left(\frac{\lambda}{4\pi R_R}\right)^2 r^2\right]^{1/2} \tag{2}$$

where the range surface must be electrically smooth at the operating wavelength (see [5, p. 14–37]).

For small grazing angles and horizonally (parallel) polarized waves the reflection coefficient approaches unity [6] so that it is acceptable to define

$$R_R = [R_r^2 + (h_r + h_t)^2]^{1/2}.$$

The factor r^2 is thus a function of the electrical and geometrical properties of the range surface, the radiation patterns of the antennas, the frequency and polarization of the transmitted wave, and the geometry of the test range.

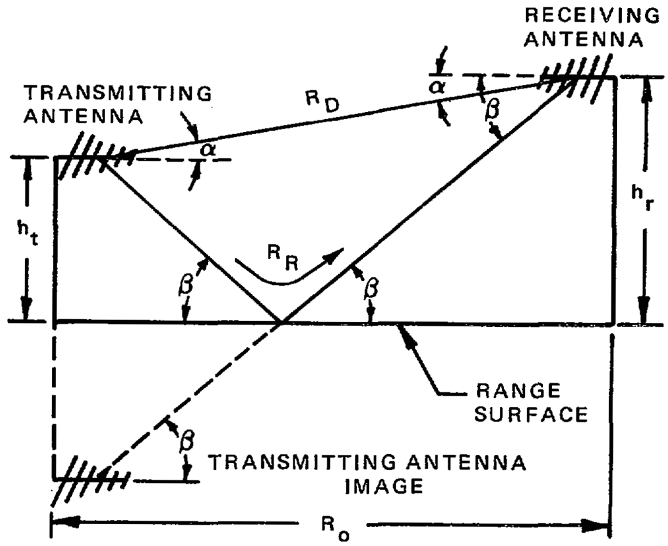

Fig. 1. Range configuration for calibrating gain of wide-beam antenna.

We will assume the antennas to be linearly polarized. It is sometimes necessary to determine the gain of an antenna which is circularly or elliptically polarized, but in such cases its gain is usually determined by the method of partial gains using a linearly polarized gain standard as a comparison.[2]

When the antenna range geometry criteria that will be given is adhered to and the antenna heights are adjusted such that the two electric-field contributions arrive in phase at the receiving antenna, the total electric field at that point, to a very close approximation over the active region of the receiving aperture, is

$$E_T = E_D + E_R \tag{3}$$

or

$$E_T = K\left[P_0G_tG_r\left(\frac{\lambda}{4\pi R_D}\right)^2\right]^{1/2}\left[(K_1K_2)^{1/2} + \frac{rR_D}{R_R}\right]. \tag{4}$$

The total received power for this in-phase case is, therefore,

$$P_r = P_0G_tG_r\left(\frac{\lambda}{4\pi R_D}\right)^2\left[(K_1K_2)^{1/2} + \frac{rR_D}{R_R}\right]^2. \tag{5}$$

Expressing (5) in logarithmic form, we have

$$L_r = L_0 + g_t + g_r - 20\log\left(\frac{4\pi R_D}{\lambda}\right) + 20\log\left[(K_1K_2)^{1/2} + \frac{rR_D}{R_R}\right]. \tag{6}$$

The gain sum $g_t + g_r$ is obtained by measuring the remaining quantities in the above equation. The only quantity which presents a significant measurement problem is the effective gain factor r^2. This factor may be determined by the following procedure.

[2] See [5, ch. 2] for further details.

First specify a height for the receive antenna such that

$$h_r \geq 4D \tag{7}$$

and

$$h_r \geq 4\lambda. \tag{8}$$

Satisfaction of these criteria ensures that the amplitude taper in the vertical plane across the receiving antenna can be made less than 0.25 dB and further ensures that mutual coupling between the receiving antenna and its image in the range surface is suppressed by at least 40 dB. These conditions will be adequate for most calibration measurements of this type.

Once this height is specified, the range length R_0 should be of sufficient length that

$$R_0 \gg 2h_r. \tag{9}$$

This requirement permits a small grazing angle (the complement of the angle of incidence) for the reflected wave. A low grazing angle is desirable for reasons that will be presented later.

In order to satisfy the in-phase criterion of (3), it is necessary that

$$h_t = \frac{(2n-1)\lambda R}{4h_r}. \tag{10}$$

For complete details see [5, ch. 14]. The transmitting antenna should be placed at the lowest position that satisfies both (10) and the mutual-coupling criterion

$$h_t \geq 4\lambda. \tag{11}$$

With the transmitting antenna in this position, the total received power is given by (5). This received power should be recorded. The transmitting antenna should then be moved to the lowest position which satisfies both (11) and the relation

$$h_t = \frac{m\lambda R}{2h_r}. \tag{12}$$

This corresponds to the location of a minimum in the interference pattern at the receiving antenna. The field at the receiving antenna is then given by

$$E_T' = E_D' - E_R' \tag{13}$$

which produces a received power of

$$P_r' = P_0 G_t G_r \left(\frac{\lambda}{4\pi R_D'}\right)^2 \left[(K_1'K_2')^{1/2} - \frac{rR_D'}{R_R'}\right]^2. \tag{14}$$

The primed quantities are defined for the new position as were the unprimed quantities for the original position. This received power should be recorded for comparison with P_r.

The effective gain factor r^2 was assumed to be the same in (5) and (14). It, in fact, differs slightly in these positions since the angle of incidence differs slightly. The quantity measured will represent an average of the values between these two positions. It is, therefore, important that the range configuration be such that the grazing angle of the reflected wave change as little as is practical between these two measurement configurations. For the criteria of (7)–(12), it is seen that the geometry which produces the smallest grazing angle also produces the smallest change in grazing angle. The limitation in choosing the smallest grazing angle is usually one of economics in the selection of range length. It is also more desirable to test at horizontal polarization than at vertical since the effective gain factor changes less rapidly with grazing angle at horizontal polarization.

Division of (5) by (14) yields

$$\frac{P_r}{P_r'} = \left(\frac{R_D'}{R_D}\right)^2 \left[\frac{(K_1K_2)^{1/2} + r\dfrac{R_D}{R_R}}{(K_1'K_2')^{1/2} - r\dfrac{R_D'}{R_R'}}\right]^2 \tag{15}$$

from which

$$r = \left(\frac{R_R R_R'}{R_D R_D'}\right)\left[\frac{[(P_r/P_r')(K_1'K_2')]^{1/2}R_D - (K_1K_2)^{1/2}R_D'}{[(P_r/P_r')]^{1/2}R_R + R_R'}\right]. \tag{16}$$

The antenna directivity quantities K_1, K_1', K_2, and K_2' should be taken from measured pattern data, based on the test geometry. Here the low grazing angle also tends to give greater accuracy because of being near the peak of the beam.

To accurately determine the various range terms, the locations of the phase centers of the two antennas must be known. Knowing their locations, one then measures their heights and the horizontal separation R_0 and calculates the direct and reflected path lengths for each configuration. Since the power terms P_r and P_r' are measured quantities, the factor r^2 is now calculiable from (16).

The received and transmitted power levels L_r and L_0 are measured with a calibrated coupling network and level meters. This procedure is then repeated three times, for three transmit–receive configurations as required for the two or three antenna method of gain calibration [3]. The resulting three simultaneous equations may then be solved for the gain of each antenna.

III. Experimental Procedure

The three-antenna method of gain calibration was implemented as shown in Fig. 2. Prior to performing the power transfer measurements several preparatory design and calibration steps were taken. First, the antenna range upon which the comparisons were to be performed was designed, constructed, evaluated, and its physical rela-

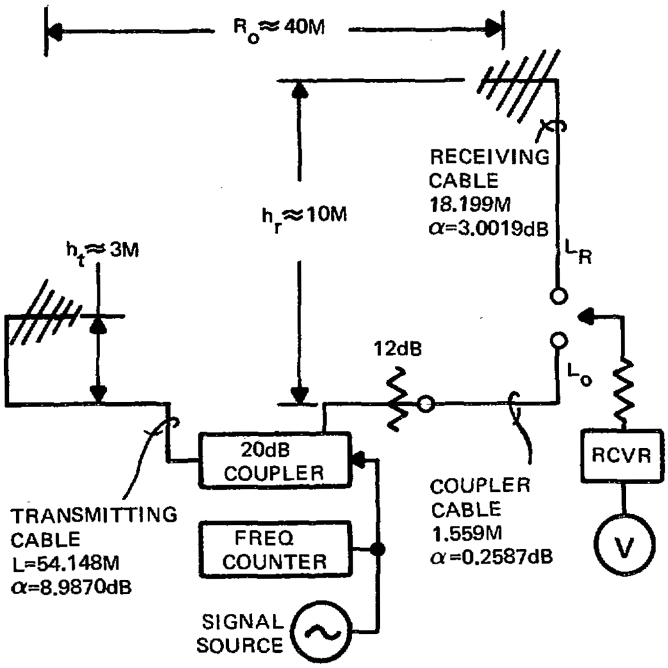

Fig. 2. Transfer measurement.

TABLE I
MEASURED DATA

A. Average Antenna VSWR and equivalent loss in dB.

Antenna	VSWR	Mismatch Loss in dB
1	1.29	0.069
2	1.30	0.073
3	1.18	0.031

B. Average Coupling Network Loss.

K[a]	dB[b]
0.02684	31.425

C. Average 60.96 m Cable Loss.

K[a]	dB[b]
0.35535	9.9870

D. Average Null Depth measurement (dB) Peak with h_t = 3.176 m.

Null with h_t = 4.532 m	Null with h_t = 2.124 m
18.22	20.42

E. Average Power Transfer in dB, h_t = 3.176 m.

Antenna Configuration				
	Transmitting	1	1	2
	Receiving	2	3	3
		13.012	12.933	12.950

[a] K is the voltage ratio as read on the Ratio Transformer.
[b] Corresponding Values in dB.

tionships carefully measured. Next, the antennas to be calibrated were designed, constructed and their parameters carefully measured. These included VSWR, pattern and phase center location.

The cable and coupler network to be used were then calibrated using a 1 kHz ratio transformer substitution

Fig. 3. UHF antenna range showing aperture field probe mounted.

technique. Finally, the power transfer measurements were made using a pattern receiver and a precision 1-kHz attenuator to determine the L_0-L_r term in the modified Friis transmission equation. For purposes of illustration of the measurement procedure, the data shown in Table I is given at 300 MHz although the antennas were calibrated at eight frequencies.

The antenna range was designed [5] and built to the following dimensions: $R_0 \approx 40$ m, $h_r \approx 10$ m, and $h_t \approx 3$ m. The range was then evaluated using aperture-field probe-measurement techniques [5]. The data indicated that the design requirements were satisfied. The UHF antenna range with the aperture field probe mounted on the receive tower is shown in Fig. 3.

The antennas choosen to be calibrated were linearly polarized log-periodic antennas consisting of eight elements of welded rod and tubular construction. The measured H-plane patterns at 300 MHz of the three antennas are shown in Fig. 4. These were measured on the ground reflection range. All of the gain comparisons were conducted with the antennas horizontally polarized, thus only H-plane data were required. The phase center locations of the log-periodic antennas were determined by calculation [7] and by measurements. The average between the two methods was selected as the phase center location. The phase center data was required to establish the range length R_0 for calculating the space dispersion factor.

The coupling network used to sample the transmit level L_0 was calibrated by the 1-kHz substitution method illustrated in Fig. 5. Also calibrated was the RF loss in a 60.96-m length of RG212/U coaxial cable.

To solve (16) for r it was necessary to measure the null depth for the out-of-phase condition as determined by the relative locations of the transmitting and receiving antennas on the ground reflection range. At the same time the height of the transmitting antenna was measured to permit the calculation of the geometrical relationships in

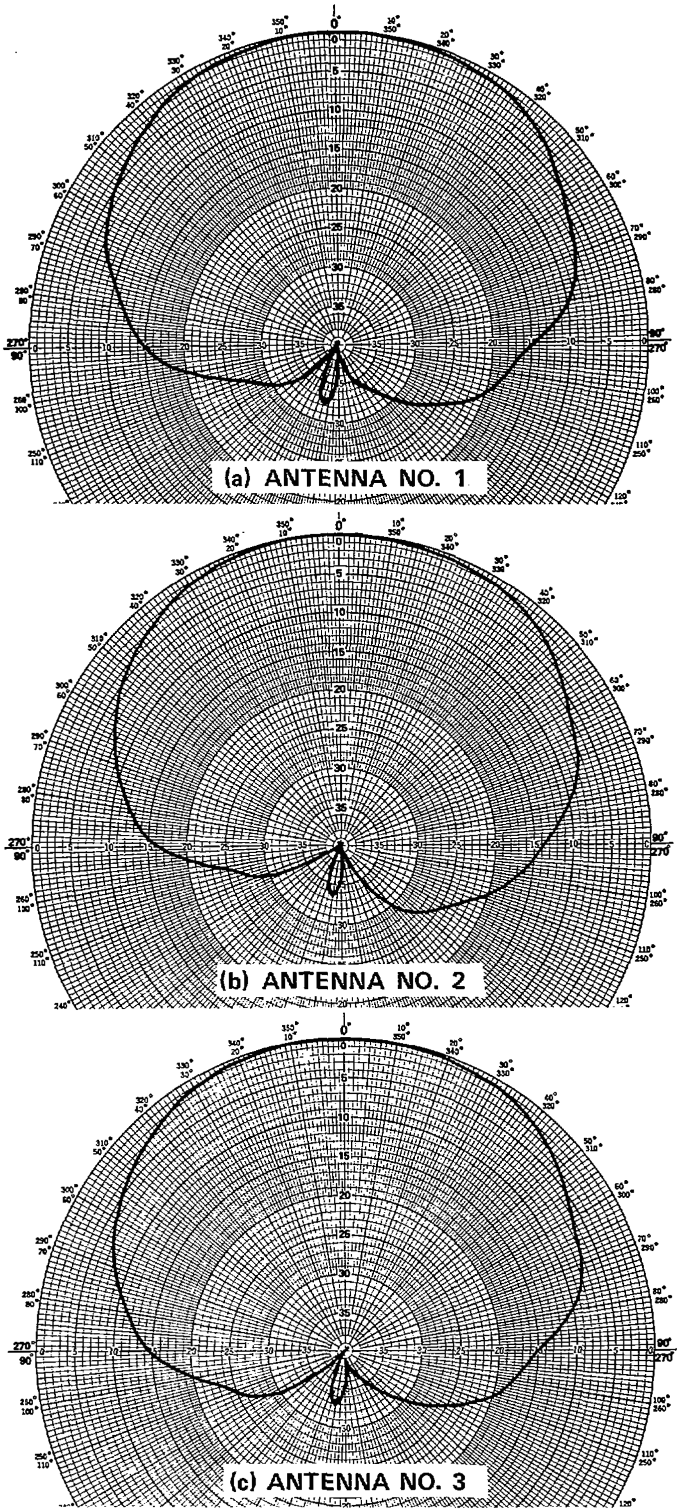

Fig. 4. H plane pattern of three UHF gain standards at 300 MHz (dB scale).

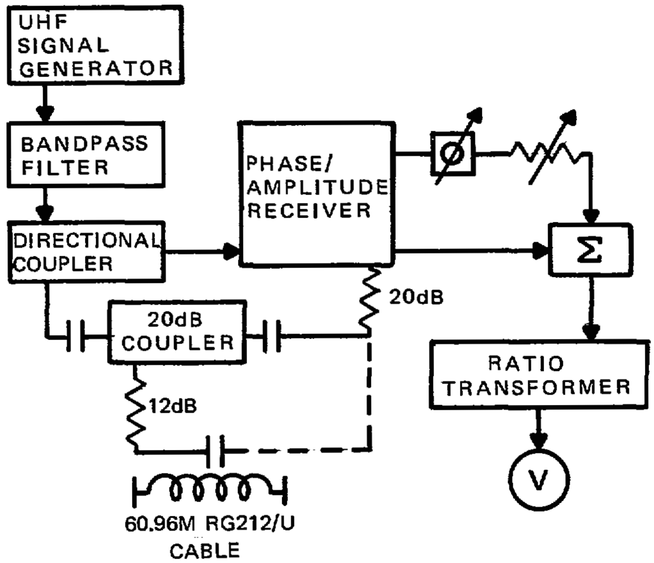

Fig. 5. Cable and coupling network loss measurement.

TABLE II
SUMMARY OF PATH ANGLE AND LOSS CALCULATIONS AS FUNCTION OF TRANSMITTING ANTENNA HEIGHT

$F = 300$ MHz $\lambda = 1$ m

		Path Length (m)	Dispersion Loss (dB)
$h_t = 2.124$ m	$\alpha = 10.41°$	$R_D = 41.575$	$S_D = 54.42$
	$\beta = 16.01°$	$R_R = 42.541$	$S_R = 54.62$
$h_t = 3.176$ m	$\alpha = 8.96°$	$R_D = 41.398$	$S_D = 54.38$
	$\beta = 17.38°$	$R_R = 42.849$	$S_R = 54.68$
$h_t = 4.532$ m	$\alpha = 7.43°$	$R_D = 41.239$	$S_D = 54.35$
	$\beta = 18.79°$	$R_R = 43.193$	$S_R = 54.75$

TABLE III
PATTERN LEVELS RELATIVE TO PEAK IN dB.

Angles in Degrees	Antennas #1 (dB)	#2 (dB)	#3 (dB)
$\alpha = 10.41$	−0.15		−0.15
$\beta = 16.01$	−0.30		−0.32
$\alpha = 8.96$	−0.10	−0.04	−0.12
$\beta = 17.38$	−0.34	−0.23	−0.40
$\alpha = 7.43$	−0.05		−0.07
$\beta = 18.80$	−0.40		−0.44

this mode of operation. See Fig. 1 and Table II. The power transfer data was obtained on the ground reflection range where the three different test antenna combinations were used as prescribed by the three-antenna method.

The angles in Table II and the pattern data given in Fig. 4 may be used to determine the pattern levels with respect to the peak of each antenna beam. The results are summarized in Table III. From the measured and calculated data the last term of (6) was solved using (16). The results of all the calculations are summarized in Table IV, where the measured and calculated data was substituted into (6) to solve for $g_r + g_t$ from which the gain of the three antennas was determined.

An estimate of the uncertainty in the calibration is given in Table V. The calibration procedure was designed to minimize major bias errors in the receivers and analog meters by holding level changes small. Large level differences were accommodated by the use of precision attenu-

TABLE IV
SUMMARY OF GAIN CALCULATIONS AT 300 MHz

Terms	Transfer Step (dB)		
	1 − 2	1 − 3	2 − 3
A. Subtract			
1) Coupling Loss	31.425	31.425	31.425
2) Coupler Cable[a]	0.259	0.259	0.259
3) Transfer Data	13.012	12.933	12.950
4) Effective Gain[b]	4.672	4.554	4.635
Subtotal	49.368	49.171	49.269
B. Add			
1) Transmitter Cable Loss[a]	8.987	8.987	8.987
2) Receive Cable Loss[a]	3.021	3.021	3.021
3) Space Dispersion Term	54.380	54.380	54.380
4) Mismatch Loss	0.070	0.070	0.073
	0.073	0.031	0.031
Subtotal	66.531	66.489	66.492
GRAND TOTAL	17.163	17.318	17.223
	no. 1	no. 2	no. 3
Antenna Gains (dB)	8.77	8.87	8.93

[a] Calculated from measured loss.
[b] Calculated results of (16).

TABLE V
SUMMARY OF ERROR TERMS (SEE TABLE IV)

Measurement	Error Component	Magnitude (dB)
Coupler, Transmit and Receive Cable Loss	Random	0.002
	Systematic[a]	0.088
Coupling Network Loss	Random	0.003
	Systematic[a]	0.055
Power Transfer	Random	0.006
	Systematic[a]	0.051
Effective Gain	Random	0.018
	Systematic[b]	0.055
Space Dispersion	Random and Systematic[c]	0.005
Mismatch Loss	Random	0.005
	Systematic[d]	0.050
	RSS	0.139

[a] Includes frequency drift, receiver linearity, ratio transformer or attenuator bias, and connector repeatability uncertainties.
[b] Includes pattern, frequency drift, receiver linearity, and intrapolation uncertainties.
[c] Includes frequency drift and distance measurement uncertainties.
[d] Includes frequency drift, connector repeatability, and equipment bias uncertainties.

ators and ratio transformers. The values given in Table V for the systematic errors include residuals which result from not being able to perform all measurements at the same operating point. An important source of uncertainty in the measurements was the making and breaking of coaxial connections during the measurements. Random errors were held small by repeating all measurements ten times. The numbers shown are the standard deviations of the means as estimated from the scatter of the individual measurements. Making the customary assumption that a Gaussian distribution applies, one can obtain a 95 percent confidence limit of ±0.27 dB by multiplying the rms resultant by 1.96.

IV. SUMMARY AND CONCLUSIONS

The method of calibrating low directivity antennas on a ground reflection range has been found to be an involved but practical method of establishing a set of standard gain antennas. The results compare favorably with those achievable at microwave frequencies when one takes into consideration the added complexity of the reflections from the range surface.

As an added note of interest, about a year later a fourth gain standard antenna was built and compared on the same antenna range to one of the calibrated standards and its gain was found to be within 0.1 dB of the original standard at all eight frequencies.

V. NOMENCLATURES

P_0	Power into the terminals of the transmitting antenna.
G_t	Maximum gain of the transmitting antenna.
g_t	Maximum gain of the transmitting antenna expressed in logarithmic form.
K_1G_t	Gain of the transmitting antenna in the direction of the receiving antenna.
G_r	Maximum gain of the receiving antenna.
g_r	Maximum gain of the receiving antenna expressed in logarithmic form.
K_2G_r	Gain of the receiving antenna in the direction of the transmitting antenna.
K	Constant of proportionality.
R_D	Direct path separation between antennas.
E_D	Amplitude of the electric field at the receiving antenna due to the direct path wave.
E_r	Amplitude of the ground-reflection electric field at the receiving antenna.
R_R	The effective path length between the receiving antenna and the transmitting antenna image.
r^2	An effective gain factor which accounts for the transfer of energy by means of reflection from the range surface.
E_T	Total electric field at the receiving antenna.
P_r	Total received power for the in-phase case.
L_r	Total received power for the in-phase case expressed in logarithmic form.
h_r	The height of the receiving antenna.
λ	The wavelength of operation.
D	The maximum aperture dimension of the receiving antenna.
R_0	Antenna range length.
n	A positive integer corresponding to the interference lobe which is peaked on the receiving antenna.
h_t	The height of the transmitting antenna.
m	A positive integer corresponding to the location of a minimum in the interference pattern at the receiving antenna.

Note: Primed quantities are used to note the conditions for a minimum in the interference pattern and unprimed quantities for a peaked interference lobe at the receiving antenna, see text for details.

α The angle between the range horizontal and the direct path signal.

β The angle between the range horizontal and the reflected path signal.

S_D Direct path dispersion loss.

S_R Reflected path dispersion loss.

Acknowledgment

The authors would like to thank the many persons who contributed to the successful completion of this project.

References

[1] E. H. Braun, "Gain of electromagnetic horns," *Proc. IRE*, vol. 41, pp. 109–115, Jan. 1953.
[2] T. S. Chu and R. A. Semplak, "Gain of electromagnetic horns," *Bell Syst. Tech. J.*, Mar. 1965.
[3] R. R. Bowman, "Field strength above 1 GHz: measurement procedures for standard antennas," *Proc. IEEE*, vol. 55, pp. 981–990, June 1967. (This paper has an excellent bibliography on the subject of antenna gain calibration.)
[4] H. T. Friis, "A note on a simple transmission formula," *Proc. IRE*, vol. 34, pp. 254–256, 1946.
[5] J. S. Hollis *et al.*, Eds., *Microwave Antenna Measurements*. Atlanta, Ga.: Scientific-Atlanta, 1970.
[6] E. C. Jordan, *Electromagnetic Waves and Radiating Systems*. Englewood Cliffs, N. J.: Prentice-Hall, 1950, pp. 629–635.
[7] R. L. Carrel, "Analysis and design of the log-periodic dipole antenna," Univ. Illinois, Urbana, AD 264 558, p. 131.

Measurement of the Radiation Patterns of Full-Scale HF and VHF Antennas

GARY E. BARKER

Abstract—**A system has been developed to measure the directivity patterns of full-scale antennas when located in their operational environments. The primary component of this system is an aircraft-towed multifrequency transmitter that is designed to approximate an elementary dipole antenna. An HF and a VHF version of this transmitter provide frequency coverage from 2 to 100 MHz. Techniques have been developed to measure the entire radiation pattern, from the horizon to the zenith, for several antennas simultaneously. Data derived from this system are processed to provide the radiation patterns as contour plots of the measured signal strength on azimuthal equal-area projections. The measurement hardware, data acquisition, and data processing techniques are described, and examples are given of measured and processed data derived from the system.**

Introduction

MATHEMATICAL and scale modeling techniques can provide some insight into the actual radiation patterns of HF and VHF antennas, but models cannot always account for all of the pattern perturbations that result from local topography, soil variations, and reflections from other antennas, power lines, or nearby metal structures. Thus full-scale pattern measurements are often required to verify pattern calculations and to determine if antennas actually produce their assumed or calculated radiation patterns when placed in their operational environments.

Manuscript received October 3, 1972; revised February 6, 1973.
The author is with the Telecommunications Department, Stanford Research Institute, Menlo Park, Calif. 94025.

The measurement technique developed by Stanford Research Institute (SRI) uses two aircraft-towed multifrequency transmitters, approximating Hertzian dipoles, to measure antenna receiving patterns. (Reciprocity is assumed when measuring the patterns of transmitting antennas.) These transmitters are described in the next section. The two basic flight patterns and data processing techniques employed to measure the antenna patterns are as follows: 1) two sets of circular orbits are flown at several elevation angles around the antenna to measure its horizontal and vertical polarization response, and 2) a grid of linear passes is flown above the antenna to determine its "power" response near the zenith. The data from these measurements are displayed as azimuthal equal-area projections of the measured antenna pattern.

Xeledop Transmitters

The unique feature of the instrumentation developed by SRI for the measurement of antenna radiation patterns is the Xeledop.[1] Two of these transmitters were designed: the HF Xeledop for 2 to 50 MHz, and the VHF Xeledop for 50 to 100 MHz [1]–[3]. Both are shown in Fig. 1.

The HF Xeledop employs eight battery-powered transmitters encased in an 11-in fiberglass sphere with two 4-ft copper radiators extending from it, each terminated by a 3-in copper ball. A ring counter is used to key

[1] Xeledop is an acronym for transmitting (Xmitting) *ele*mentary *d*ipole with *o*ptional *p*olarization.